Track core size estimation for heavy ions in CR-39 by AFM and UV methods

Yamauchi, Tomoya ; Yasuda, Nakahiro ; Asuka, Taku ; Izumi, Kentaro ; Masutani, Takashi ; Oda, Keiji ; Barillon, Remi

IRaP2004 (P-046)

Track core size estimation for heavy ions in CR-39 by AFM and UV methods

T. Yamauchi[a,*], N. Yasuda[b], T. Asuka[a], K. Izumi[a], T. Masutani[a], K. Oda[a], R. Barillon[c]

[a] Faculty of Maritime Sciences, Kobe University, 5-1-1 Fukaeminami-machi, Higashinada-ku, Kobe 658-0022, Japan.

[b] National Institute of Radiological Science, 4-9-1 Anagawa, Inage-ku, Chiba 263-8555, Japan.

[c] Institut de Recherches Subatomiques, Universite Louis Pasteur (UMR 7500), 23 rue du Loess, Strasbourg Cedex-2 67037, France

Abstract

The radial core size of tracks in CR-39 plastics has been determined for several heavy ions, O(8.6 MeV), Ne(18.8 MeV), Si(27 MeV) Ar(35 MeV) and Fe(80 MeV), by AFM and UV methods. In the AFM method, the core radii were assessed from the growth behavior of minute etch pits within 1 min of etching. These were derived from each intersection of the extrapolated line, fitted to each growth curve of etch pit radius. With the UV method, changes in the UV-visible spectra of CR-39 with fluence were obtained. Then the critical fluence where the track overlapping became statistically significant was determined for each ion. Based on the track overlapping model, the track core radius was calculated. Both methods were found to give results concordant with each other for these heavy ions.

PACS: 07.79.Lh; 33.20.Lg; 61.80.jh; 61.82.Pv

Keywords: Latent track; Track core size; CR-39; AFM; UV-visible; track overlap

*Corresponding author. Fax +81 78 431 6369;

e-mail: yamauchi@maritime.kobe-u.ac.jp

1. Introduction

This is the second report resulting from a more general study on the track core size in CR-39 plastics, poly-diethylene-glycol bis(allylcarbonate), using the AFM and the UV methods. The CR-39 is well known as the most sensitive etched nuclear track detector for more than 25 years [1]. However, there are some unresolved aspects in the track formation process occurring in this material [2]. Determination of the radial size of the latent tracks in CR-39 should be one of the important objects in order to understand the track formation mechanism [3,4].

In the AFM method, series of etch pit growth curves, plotting of pit radius against etching time, were obtained through the surface morphological observation using an Atomic Force Microscope (AFM) during the early stage of chemical etching [5-7]. Extrapolating the growth curves toward the origin of etching time, the coordinates of the intersections of pit radii were regarded as the track core size, where significant radial track etching should have occurred. In the UV method, series of UV-visible spectra of irradiated CR-39 were attained as a function of the ion fluence [2, 8, 9]. Then the track core size was assessed from the fluence dependence of the UV spectra based on a suitable model for track overlapping.

In the present study, these two methods have been found to derive concordant results for the radial core size of tracks in CR-39 formed by heavy-ion irradiation in air. Track dose model by Katz indicated that the track cores were produced at regions where the local dose was higher than several hundred kGy [3].

2. Materials and experiments

CR-39 of BARYOTRAK (Fukuvi Chemical Ltd., Japan) with thickness 950 μm was utilized in this study. It was made from purified monomers with a degree of purity higher than 99.9 %.

Gamma-irradiation was made at the Institute of Scientific and Industrial Research, Osaka University. Heavy-Ion exposure with O(8.6 MeV), Ne(18.8 MeV), Si(27 MeV) Ar(35 MeV) and Fe(80 MeV) was performed at HIMAC, NIRS, Japan. For the AFM observation, the range of fluence was between 10^8 and 10^9 ions/cm^2, depending on the duration of the following chemical etching. Subsequent to the slight chemical etchings in a stirred 6N KOH solution at 70 ºC, the surface observation was performed using AFM. Our AFM (OLYMPUS NanoVision 2000, Japan) was operated

in the tapping mode using an OLYMPUS Micro Cantilever tip. For the samples of the UV-visible observation, the fluences ranged from 10^{10} to 10^{13} ions/cm^2, depending on the ion species. The UV-visible absorbance was determined with a conventional spectrometer (SHIMADZU Corp., model UV-1600PC). Each measurement was done several days after the exposures.

3. Results and discussion

3.1. Track core radius from AFM method

The evolutions in pit radius for heavy ions are shown in Fig. 1 as a function of the etching time. The data points are the averages over more than 10 measurements of etch pits, and the error bars correspond to the standard deviations. Each line was attained by a least-square fit. As shown in this figure, the fitted line does not pass through the origin. The coordinates of the intersection should represent the track core radii at regions where the radial track etch rate is significantly increased [4]. The core radii obtained for these ions are summarized in Table 1. The stopping power listed in this table was calculated using the StopPow program [10].

3.2. UV spectra of gamma-irradiated CR-39

Changes in the UV-visible spectra of CR-39 exposed to gamma-rays (Co-60) with the absorbed dose are shown in Fig. 2, at doses ranging from 1 kGy to 2 MGy [8, 9]. The fraction of absorption at larger wavelengths became significant with increasing dose in general. We found that the samples had colored like amber at higher doses. Two distinct absorption bands were observed around 240 nm (1st peak) and 280 nm (2nd peak). The 1st peak increased in height significantly up to 100 kGy, and was then saturated. On the other hand, the 2nd peak increased in height at larger doses above 100 kGy. Such dose dependence of the spectra should relate to the changes in the chemical structure of irradiation damage in CR-39. In order to point out the characteristics of the damage more clearly, the height ratio of the 2nd to the 1st peak as a function of the dose is plotted in Fig. 3. This ratio has an almost constant value up to about 20 kGy, while the optical density increases proportional to the dose. We think that only the number of the identical micro-damage zones should increase and the structure of each micro-damage produced by an interaction with gamma-rays hardly changed at these lower doses (indicated as “Phase 1” in Fig. 3). Above the dose of 20 kGy, the ratio increased

significantly ("Phase 2"), and then saturated for more than 1 MGy. The micro-damage occurring during the early stage of the irradiation would be modified to other types of damage by the following irradiation. Higher values for the ratio of the peak height could result from such modified severe damage by absorption of a higher dose. It is another important issue to identify the structure of the micro-damage by low-LET radiation [3].

3.3. UV spectra of CR-39 irradiated by heavy ions and the critical fluence

Contrary to the uniform energy deposition by gamma-rays, the radiation energy is deposited locally along the track in the case of heavy ions. As a typical example, the UV spectra of CR-39 exposed to Ne ions are shown in Fig. 4. By increasing the fluence, the absorption was raised at all wavelengths. To clarify the fluence dependence of the spectra, the absorbance at the 1st and 2nd peak is plotted as a function of the fluence in Fig. 5. As shown in this figure, the absorbance at the 1st peak is proportional to the fluence up to 4×10^{11} ions/cm^2. This implies that the track overlapping became significant above this critical fluence. Without over-lapping, all tracks are characterized by an equal chemical structure and radial distribution of color centers. At lower fluences where the overlapping is negligible, the optical absorbance of the irradiated CR-39 will be simply proportional to the fluence. Based on the track overlapping model, that was described elsewhere [2,6,8,9], this critical fluence can be converted to the core radius of 3.4 nm (2.9-4.8 nm). The values inside the parentheses mean a possible distribution of core radius.

3.4. Track core radius

In the same way, the core radii for O, Si, Ar and Fe ions were assessed from their series of UV-spectra to be 3.2 nm (2.5-4.1 nm), 4.0 nm (3.2-5.3 nm), 4.0 nm (3.2-5.3 nm) and 5.0 nm (4.0-6.7 nm), respectively. In Fig. 6, the obtained track core radii are shown as a function of the averaged stopping power along the trajectory. And the two ends of the error bars in lateral direction are the maximum at the Bragg peaks and the values at the surface (For Fe ions, we simply give the lower end as a half of stopping power at the Bragg Peak) [10]. The solid curve is the best fit to the points in the form of the power function, written as,

$$r_t = 0.214 \left(\frac{dE}{dx} \right)^{0.38}, \quad \text{in nm,} \qquad (1)$$

where *dE/dx* is expressed in units of keV/μm. This agrees with our previous results for lighter ions, protons, He, C and O ions, obtained after irradiations in vacuum [2,6]. In Fig. 7, the track core radii resulting from the AFM observations listed in Table 1 are shown as a function of stopping power on the sample surface, as well as the curve by Eq. (1). The results from the AFM method are slightly larger than those from the UV method. But they are concordant with each other within the experimental errors.

3.4. Local dose around the core

The radial-dose-distribution theory for ion tracks enables us to calculate the local dose around the radius of the track core [3]. Fig. 8 shows radial dose distributions for O(8.6 MeV) and Fe(80 MeV) ions. At the core radius of the O ion from the AFM method, the corresponding local dose is 765 kGy. The end points of the error bar correspond to 461 and 1330 kGy, respectively. In the case of Fe ions, the local dose is 249 kGy with a distribution between 109 and 860 kGy. The results for other ions are listed in Table 1. These calculations indicate that the track core is formed at a region where the local dose is larger than a several hundred kGy. It is noteworthy that the fraction of the 2nd peak in UV spectra of gamma-irradiated CR-39 increases drastically at this dose region (See Figs. 1&2, higher doses in "Phase 2"). The corresponding chemical modification in the track core should be examined to understand the track formation process in CR-39 [2,7].

Acknowledgement

We would like to express our thanks to the staff of NIRS-HIMAC for their support during the experiments (14P138). This work was carried out as a part of the Research Project with Heavy Ions at NIRS-HIMAC. Thanks are also due to Mr. T. Ikeda, Dr. Y. Honda and Prof. S. Tagawa, Osaka University, for their help in gamma-ray irradiation.

References

[1] B.G. Cartwright, E. K. Shirk and P.B. Price, Nucl. Instr. and Meth. 153 (1978) 457.

[2] T. Yamauchi, Radiat. Meas. 36 (2003)73.

[3] M.P.R. Waligorski, R.N. Hamm and R. Katz, Nucl. Tracks Radiat. Meas. 11 (1986) 309.

[4] W. Enge, Radiat. Meas . 25, (1995) 11.
[5] N. Yasuda, K. Uchikawa, K. Amemiya, N. Watanabe, H. Takahashi, M. Nakazawa, M. Yamamoto, K. Ogura, Radiat. Meas. 34 (2001)45.
[6] T. Yamauchi, D. Mineyama, H. Nakai, K. Oda, N. Yasuda, Nucl. Instr. and Meth. B208 (2003) 145.
[7] T. Yamauchi, A. EL-Rahmany, D. Mineyama, H. Nakai, K. Oda, Radiat. Meas. 37 (2003)119.
[8] T. Yamauchi, T. Taniguchi and K. Oda, KEK-Proceedings 99-8 (1999) 45.
[9] T. Yamauchi, H. Ichijo and K. Oda, Proc. The First International Symposium on Supercritical Water-cooled Reactors, 407 (2000) 274.
[10] B. Doerschel and J. Henniger, Nucl. Instr. and Meth. B171 (2000) 423.

Table 1. Track core radius from the AFM method and local doses.

Ion	Energy (MeV)	dE/dx (keV/μm)	Core radius (nm)	Dose (kGy)
O	8.6	1530	2.84 ± 0.76	765 (461-1330)
Ne	18.8	1480	4.18 ± 1.18	353 (265-800)
Ar	35	3180	5.61 ± 1.13	365 (219-664)
Fe	80	4640	7.32 ± 2.66	249 (109-860)

Figure Captions

Fig. 1. The evolution of etch pit radius for O(8.6 MeV), Ne(18.8 MeV), Ar(35 MeV) and Fe (80 MeV) ions at early stage of chemical etching within 1 min.

Fig. 2. UV-visible spectra of gamma-irradiated CR-39. The fraction of absorption at larger wavelength becomes significant at higher doses.

Fig. 3. Changes in the peak height ratio of 2nd peak (280nm) to 1st peak (240nm) of gamma-irradiated CR-39.

Fig. 4. UV-visible spectra of CR-39 exposed to 18.8 MeV Ne ions.

Fig. 5. Changes in the absorbance of CR-39 irradiated by 18.8 MeV Ne ions at the 1st (240nm) and 2nd (280nm) peaks.

Fig. 6. Relation between the track core radii and stopping power from the UV method.

Fig. 7. Comparison of track core radii from the AFM method and the UV method in CR-39 plastics.

Fig. 8. Radial dose distribution for C and Fe ions.

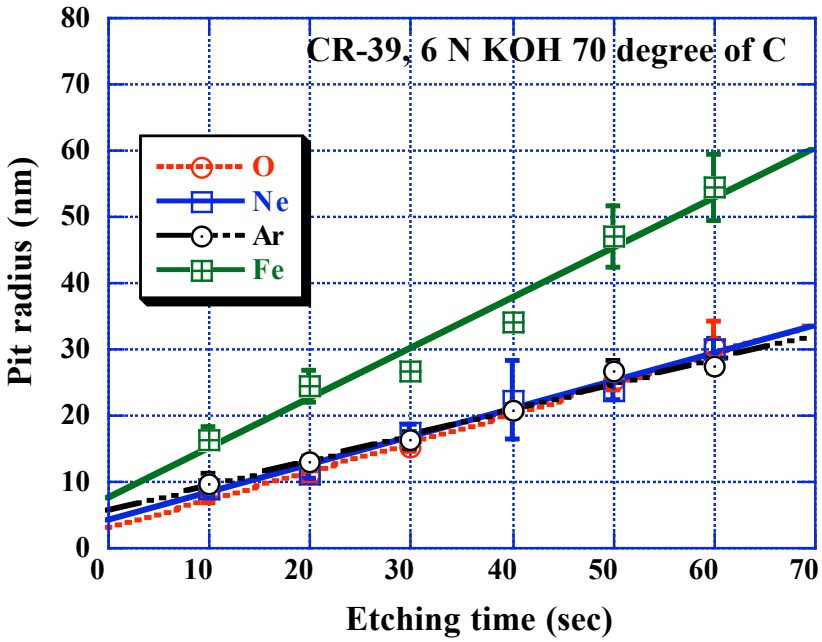
CR-39, 6 N KOH 70 degree of C
O
Ne
Ar
Fe
Pit radius (nm)
Etching time (sec)
0
10
20
30
40
50
60
70
80

Fig. 1

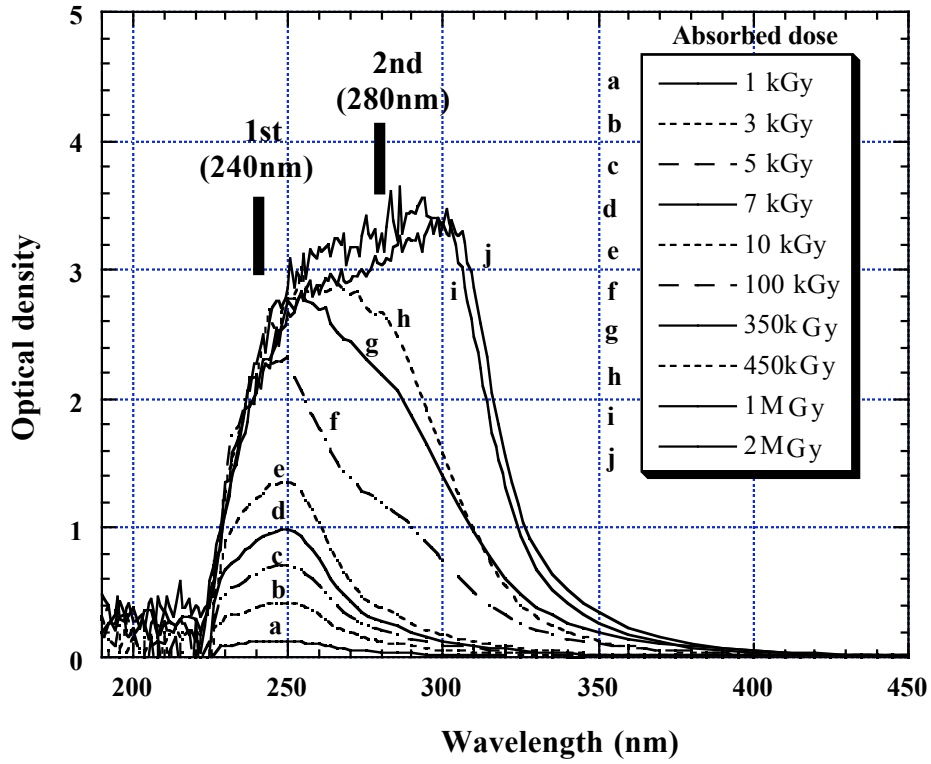
Optical density
Wavelength (nm)
0
1
2
3
4
5
200
250
300
350
400
450
1st
(240nm)
2nd
(280nm)
Absorbed dose
a 1 kGy
b 3 kGy
c 5 kGy
d 7 kGy
e 10 kGy
f 100 kGy
g 350k Gy
h 450kGy
i 1MGy
j 2MGy

Fig.2

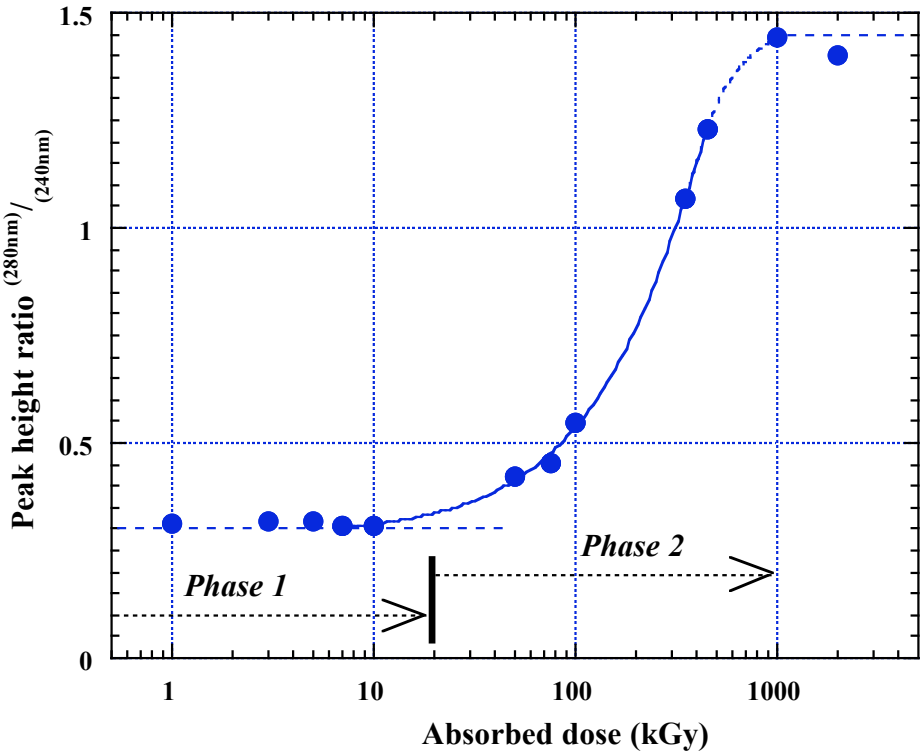
1.5
1
0.5
0
Peak height ratio (280nm)/(240nm)
1
10
100
1000
Absorbed dose (kGy)
Phase 1
Phase 2

Fig. 3

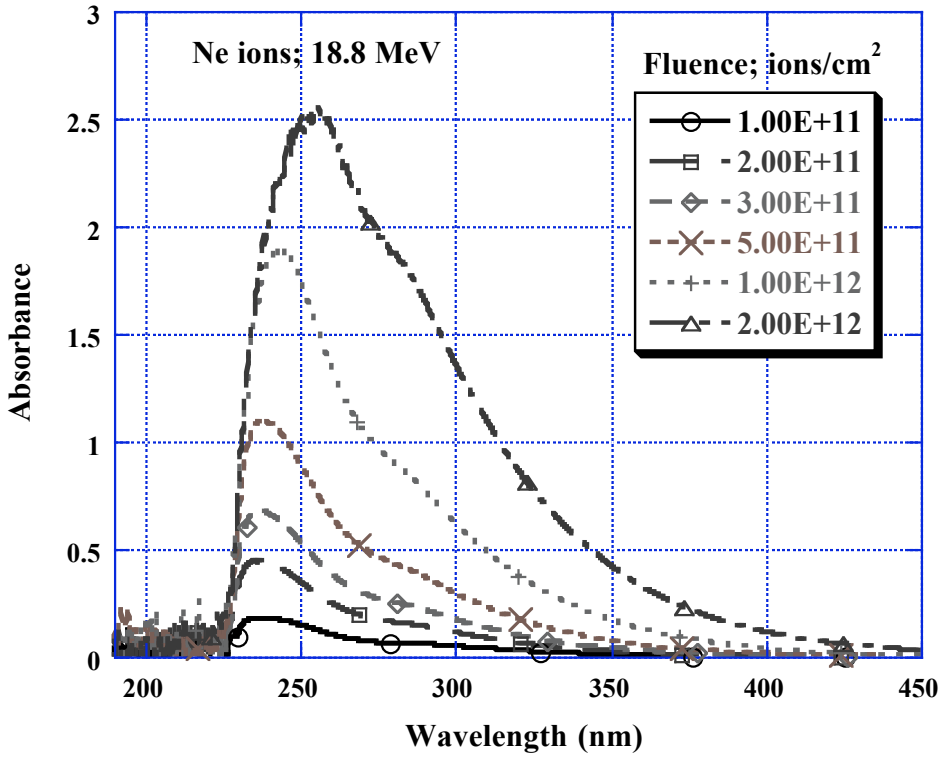
Ne ions; 18.8 MeV
Fluence; ions/cm2
1.00E+11
2.00E+11
3.00E+11
5.00E+11
1.00E+12
2.00E+12
Absorbance
Wavelength (nm)
0
0.5
1
1.5
2
2.5
3
200
250
300
350
400
450

Fig. 4

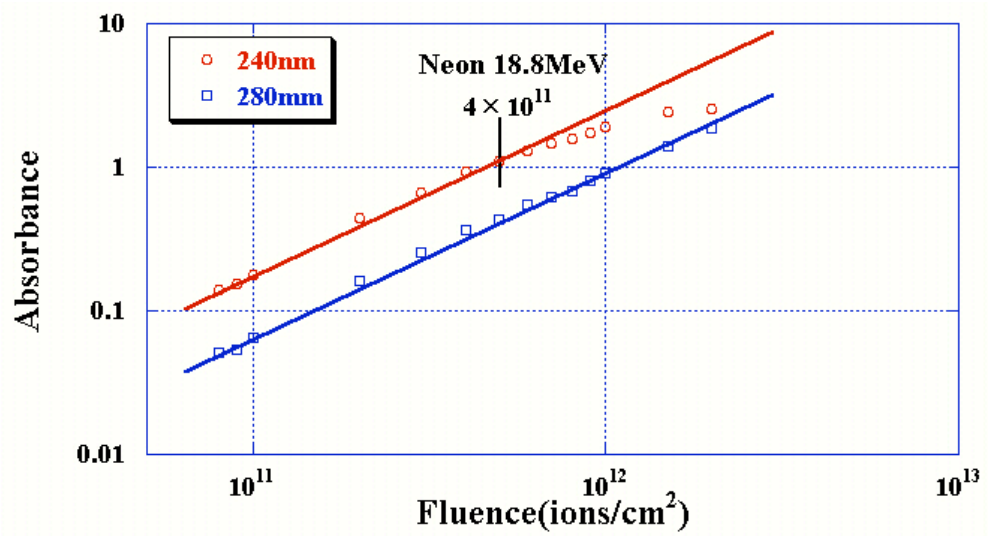
10
1
0.1
0.01
Absorbance
240nm
280mm
Neon 18.8MeV
4 × 10^11
10^11
10^12
10^13
Fluence(ions/cm^2)

Fig. 5

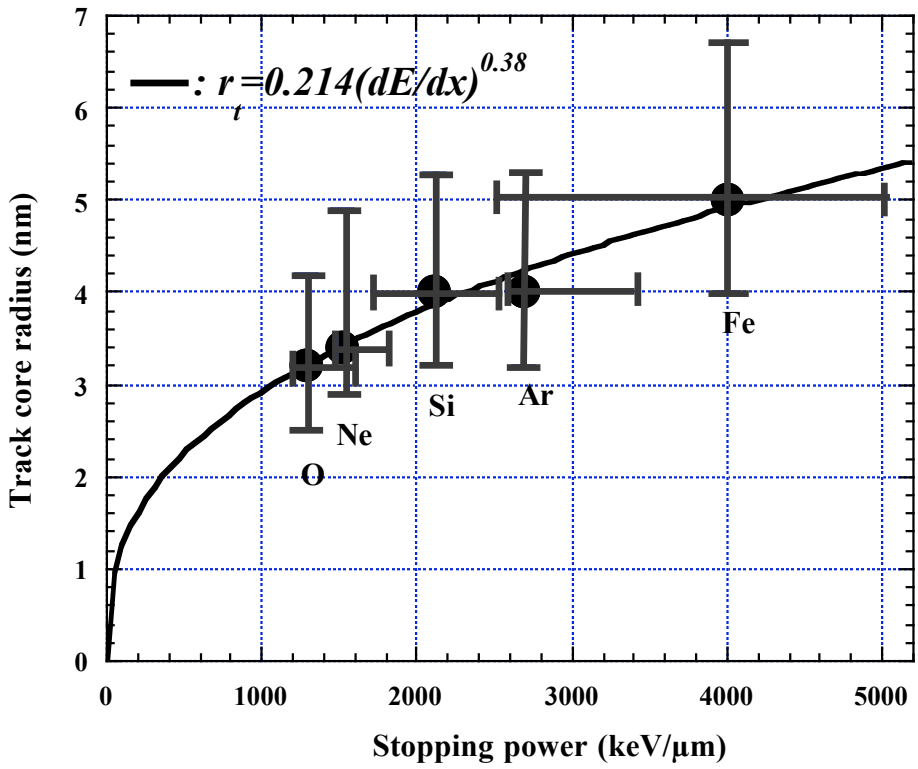
: $r_t = 0.214(dE/dx)^{0.38}$
Track core radius (nm)
Stopping power (keV/μm)
0
1
2
3
4
5
6
7
0
1000
2000
3000
4000
5000
O
Ne
Si
Ar
Fe

Fig. 6

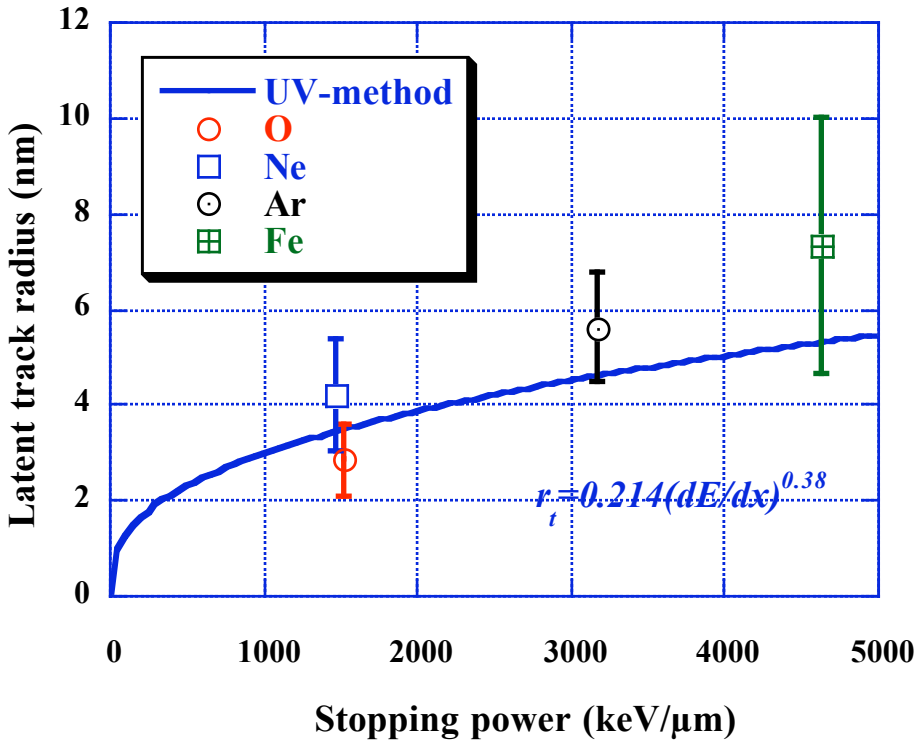
12
10
8
6
4
2
0
Latent track radius (nm)
UV-method
O
Ne
Ar
Fe
$r_t = 0.214(dE/dx)^{0.38}$
0
1000
2000
3000
4000
5000
Stopping power (keV/µm)

Fig. 7

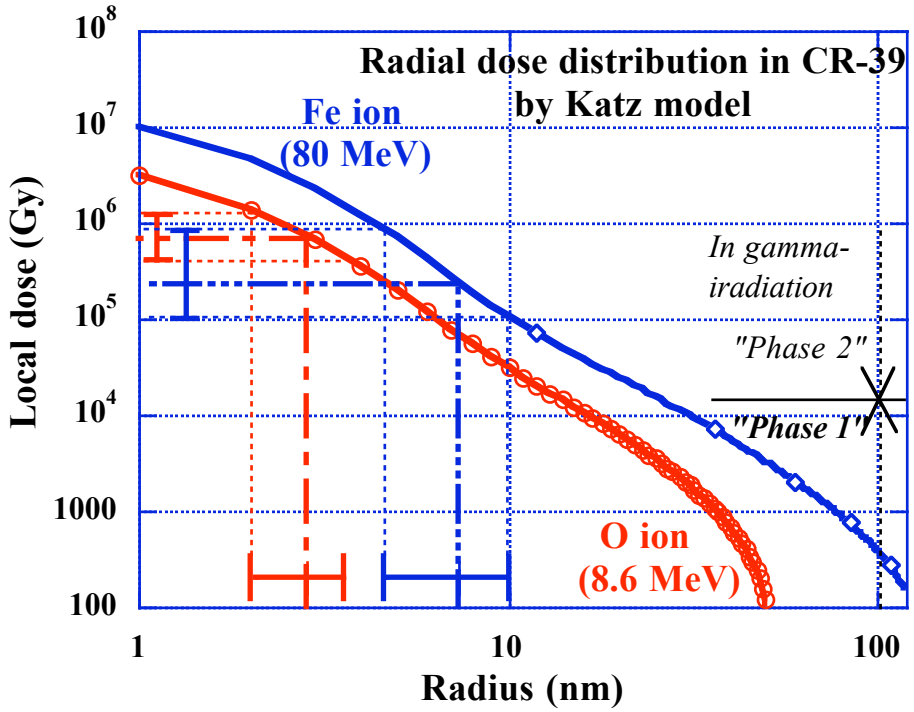
Radial dose distribution in CR-39
by Katz model
Fe ion
(80 MeV)
O ion
(8.6 MeV)
In gamma-
iradiation
"Phase 2"
"Phase 1"
Local dose (Gy)
Radius (nm)
10^8
10^7
10^6
10^5
10^4
1000
100
1
10
100

Fig. 8